

# Combined Experimental and Analytical Model of the Lumbar Spine Subjected to Large Displacement Cyclic Loads Part II—Model Validation

Naira H. Campbell-Kyureghyan<sup>1</sup> and William S. Marras<sup>2</sup>

<sup>1</sup>University of Louisville, Department of Industrial Engineering, JB Speed Building Room 308, Louisville, KY 40292

<sup>2</sup>The Ohio State University, Department of IWSE, 1791 Neil Ave., 210 Baker Systems, Columbus, OH 43210

---

*A two-dimensional model has been developed that calculates the motion and forces within the lumbar spine during sagittal lifting tasks. The model integrates computations with measured motion to provide near real-time predictions of large displacement behavior. Full validation of the individual model components as well as the full model was performed. The individual components were found to accurately reproduce the full range of reported behavior using typical material properties and geometries. Five minutes of continuously measured and calculated results were used to validate the complete model. The motion and component forces were validated against the available data in the literature. The ability of the model to capture spatial variations in response is demonstrated through both stress distributions within a disc and the deviation in component forces between disc levels.*

**Keywords:** Lumbar spine; Finite element analysis; Biomechanical modeling; Dynamic motion; Cyclic loading; Model validation

---

## 1. INTRODUCTION

Detailed knowledge of the behavior of the lumbar spine under normal and abnormal postures and loading can lead to improved work design and clinical therapies. One path to obtaining this knowledge is biomechanics. Obtaining experimental data, particularly at or near the injury threshold, is problematic both practically and ethically. Analytical approaches such as finite element modeling (FEM) provide valuable insight into spinal behavior and can be applied to a wide range of situations. However, in order for the model results to be useful the model must be validated against experimental results.

Twenty five studies from 1980 onwards were reviewed with respect to their validation studies and other factors. Only three of the models included the entire lumbar spine (Pankoke, *et al.*, 1998; Kong, *et al.*, 2003; Ezquerro, *et al.*, 2004) and the model from Pankoke *et al.* is extremely simplified, lumping the entire intervertebral disc into an equivalent spring and dashpot. Nine of the studies used complex loads with compression, shear, and/or flexion applied simultaneously. Dynamic loads were applied in nine of the studies, but five of those were creep tests where the load was applied and held constant over time, and three of the remaining four were vibration studies at high frequencies, with the last study (Lee *et al.*, 2000) applying an impact load. Two of the three vibration studies (Goel *et al.*, 1994; Pankoke *et al.*, 1998) were also the only ones to consider cyclic loads,

but the loads were not representative of those encountered during actual motions.

Parametric studies were partially performed in nine of the studies. Typically, a single parameter was varied over a limited range and the effect on one or two output quantities was examined. None of the studies performed a full parametric analysis, including even a significant number of the myriad model parameters. Four of the studies partially validated the results. A limited number of model results were compared to experimental data. For example, Shirazi-Adl *et al.* (1986) validated their torque-axial rotation results, but the torques applied to the model far exceeded the measured values. Lee *et al.* (2000) compared the axial strain variation in the cortical shell and the creep response to a single experimental result. Out of twenty five reviewed papers, only three (Lu *et al.*, 1996; Pankoke *et al.*, 1998; Ezquerro *et al.*, 2004) included more complete validation studies, with multiple model results compared to several measured values. For example, Ezquerro *et al.* (2004) validated the motion segment stiffness in four modes (compression, shear, flexion, torsion) against up to four reported experimental results.

In the companion article (Part I) to this paper we describe a model that is able to capture the large displacement cyclic motion of the lumbar spine. The model contains elements for each major component of the spine. The elements were developed to capture the essential behavior that affects the overall motion, as well as provide some critical detailed results to help pinpoint

the areas of particular interest for evaluating damage. The model is linked to experimentally measured sagittal flexion motions. The advantage of this model is that it is capable of predicting the lumbar spine behavior subjected to realistic loads in near real-time.

The objective of this study was to verify the validity of the components and complete model. The component validation uses existing experimental results to compare with the model predictions. Since it is not possible to directly measure the forces and deformations within the lumbar spine during motion, the overall model validation uses the limited existing experimental values along with extrapolations of reported behaviors. In addition, a full parametric analysis of the primary input variables was performed to determine their importance in the response, and to verify the ability of the model to correctly capture the full range of reported behaviors.

## 2. MODEL DESCRIPTION

The lumbar spine model is briefly described in this section. A complete description is contained in the companion paper. The finite element model validated and applied in this paper bridges the gap between complex finite element models and simplified models providing little behavioral detail. The major components of the lumbar spine are explicitly modeled at a level of detail sufficient to provide results indicating the stress, strain, and their sources within the components, but still allowing for near real-time calculation of the large displacement dynamic motion. The model is explicitly linked to experimentally recorded flexion motions to provide the basic loading input.

The model includes vertebral bodies, endplates, posterior elements, ligaments, and intervertebral discs. Six vertebral bodies are included in the model, L<sub>5</sub> (lumbar) -T<sub>12</sub> (thoracic) along with their endplates and posterior elements. Six discs are placed between the endplates and a variable number of ligaments may be included in the model. The resulting model has thirteen nodes and 37 degrees of freedom with the sacrum (S) fixed against translation as a reference point.

The load (displacement) is applied at the top of T<sub>12</sub> using output from the Lumber Motion Monitor (LMM) during sagittal lifting tasks. The relationship between the LMM motion and the displacement of T<sub>12</sub> has been determined previously (Campbell-Kyureghyan, *et al.*, 2005). The calculation proceeds in three phases. In the first phase the subject specific model is derived based on anthropometric measurements and preliminary LMM measurements. The second and third phases involve the calculation of the dynamic motion. At each step the position of T<sub>12</sub> is determined based on the LMM readings and applied to the model. The remaining degree of freedom motions are then calculated and used to

determine the component deformations and stresses. Finally, the model properties are updated using the current geometry and component stiffness values.

## 3. MODEL VALIDATION

In any type of modeling, choosing the correct parameter values is of paramount importance. For biomechanical models, the material properties are the parameters that have the most effect on the results. Each run of a model uses a single number for each property. However, the inherent variability of biological tissue leads to a range of feasible properties, not a single known or estimated value. The properties can vary both between individuals and within a single person, and can also be influenced by age, time, and even gender. It is therefore imperative that any model be validated against the available data, and be able to reproduce the full spectrum of possible behavior(s) (Fagan *et al.*, 2002). This section briefly summarizes the results of the validation studies documented elsewhere (Campbell-Kyureghyan, 2004). Material properties from the literature, summarized in Table 1, were used as the baseline for the model validation and examples.

**Table 1**  
Material and geometric properties used for model validation and examples

Material	Elastic Modulus (MPa)	Damping Coef. (MPa-s)	Area (mm <sup>2</sup> )
Cancellous Bone	100	-	804
Cortical Bone	10000	-	103
Endplates	250	-	907
Disc Nucleus	10	0.10	653
Ground Substance	8.4	0.01	611
Collagen Fibers	500	0.01	153
Ligaments	3.4-13	0.01	20-63.7

**Ligaments.** Ligaments are collagenous tissue and consist mostly of type I collagen, which are tension resistant (Bogduk, 1997). Usually ligaments exhibit a behavior similar to isolated collagen fibers, which is characterized by a stress-strain curve (Shah *et al.*, 1977; Shah, 1980; Nordin and Frankel, 2001) that is divided into four functional regions: a silent zone, transition or toe, linear and yield (Figure 2 in Part I). The equation used, in this study, to model the behavior is

$$E = \{1.0 + \tanh(\psi[\varepsilon - \varepsilon_0])\} \{ (E_{\text{taut}} - E_{\text{slack}}) / 2.0 \} + E_{\text{slack}}$$

where  $E_{\text{taut}}$ , the tangent modulus at large tensile strains,  $\varepsilon_0$ , the center strain of the ligament modulus transition ("activation" strain), and  $\psi$ , a factor defining the shape of the transition curve, are the parameters of interest.

Biological materials also exhibit dependence on the frequency (rate) of the applied load. With the same magnitude of load applied, but at different rates, ligaments will exhibit different behavior. In addition, the loading curve changes with each cycle, quickly at first and then gradually becomes stable (Tkaczuk, 1968). The impact of hysteresis on ligament behavior reveals a gradual diminishing in tension and joint laxity, therefore altering the risk of injury (Solomonow, 2004). To address the above issues, the performance of the ligament model was examined for both monotonic and cyclic behavior.

**Monotonic Behavior:** Multiple studies, both experimental and analytical, examined the monotonic behavior of ligaments under tension. Four of those studies provided sufficiently detailed information on the properties of interest for the current model to be used for comparison and validation. Goel *et al.* (1994) and Lu *et al.* (1996) present models, tailored to each lumbar spine ligament, that were derived considering previous experimental studies. Shirazi-Adl *et al.* (1986) describes a curvilinear ligament model, also derived from earlier studies. Finally, Chazal *et al.* (1985) provide detailed experimental results for tensile loading of the lumbar ligaments.

The values of the taut elastic modulus ( $E_{taut}$ ) and the strain at which the transition between slack and taut is centered ( $\epsilon_0$ ) are presented in Table 4.1 for all four studies. The values  $E_{taut}$  and  $\epsilon_0$  vary widely, not only between studies but also between the different ligaments. The validation of the model for each ligament starts by assuming a value of  $E_{taut}$  equal to that presented in Table 2 for the each model and ligament. The values of  $\epsilon_0$  and  $\psi$  in the model were then varied to match the stress and strain at Points A and B (in Figure 2 of Part I). Choosing the correct values of  $\epsilon_0$  and  $\psi$  allowed the model to match the experimental data from both studies.

**Table 2**  
**Values of taut modulus ( $E_{taut}$ ) and center strain of the transition zone ( $\epsilon_0$ ) from experimental studies**

Parameter	Ligament	Study			
		Chazal (1985)	Shirazi-Adl (1986)	Goel (1994)	Lu (1996)
$E_{taut}$ (MPa)	ALL	24.875	110.6	20	20
	PLL	61.6	110.6	20	70
	LFL	104	64.6	19.5	50
	ITL	556	110.6	58.7	50
	ISL	36.3	118.9	11.6	28
	CL	-	118.3	32.9	20
	SSL	36.3	110.6	15.0	28
	$\epsilon_0$	ALL	0.12	0.197	0.12
PLL		0.11	0.197	0.11	-
LFL		0.06	0.421	0.062	-
ITL		0.085	0.197	0.18	-
ISL		0.12	0.139	0.14	-
CL		-	0.304	0.25	-
SSL		0.12	0.197	0.20	-

The shape of the transition zone between slack and taut is relatively consistent between data sets, hence the values of  $\psi$  were consistent for a given ligament. However, the strain at which the transition occurs varied widely (see Table 2), leading to vastly different values of  $\epsilon_0$ . Therefore, although it has been shown that the model used in the present study can accurately reproduce the available data over its entire range, the data does not lend itself to a consensus choice of parameters, at least for  $\epsilon_0$  and  $E_{taut}$ . Therefore, final values for the monotonic behavior parameters were obtained by evaluating all available data against biological feasibility and are presented in Table 3.

**Table 3**  
**Values of parameters for ligament model chosen based on validation study**

Ligament	$\psi$	$\epsilon_0$	$E_{taut}$
ALL	23.5	0.02	7.8
PLL	17.6	0.02	10.0
LFL	10.2	0.45	7.5
ISL	18.4	0.15	13.0
SSL	16.4	0.22	3.4

**Cyclic Behavior:** There is very little data concerning the cyclic behavior of ligaments. A single study by Tkaczuk (1968) presents data showing the change in behavior over three cycles. The major findings of this study were that ligaments stiffen with cycling, and the hysteretic energy dissipation (measured by the area between the loading and unloading curves) decreased. The hysteretic energy dissipation is of particular importance since it is commonly used as a damage measure (Lee, 1999; Kunnath *et al.*, 2004; Yoshida *et al.*, 2004).

The energy dissipation is captured in the model using a dashpot in parallel with the nonlinear spring representing the elastic ligament behavior. Values of  $E_{taut}$  of 59.6 MPa and 216.2 MPa,  $\epsilon_0$  values of 0.16 and 0.099, and  $\psi$  values of 12.5 and 45 were chosen for cycles one and three respectively based on the reported stress-strain curves. Parametric analyses investigating the effect of the transition zone center strain and damping parameter on the energy dissipation over a single cycle were performed. The damping parameter had a major effect on the energy dissipation as expected. Energy dissipation also showed a strong dependence on the transition zone center strain with a difference of 60% over the reported range of  $\epsilon_0$ .

**Dynamic Behavior:** Strain rate has been found to influence both the stiffness and fatigue life of biological tissue (Martin *et al.*, 1998). The change in stiffness that occurs as the loading rate increases for a supraspinous

ligament was investigated by Solomonow (2004). In this study, the strain rate was increased from 25% strain per second to 200% strain per second, resulting in stress increases up to approximately 50%.

The increase in stress due to higher strain rates was calculated and compared to the data from Solomonow (2004). The basic ligament stress-strain curve derived above for the study of energy dissipation was used. The ultimate value of damping parameter,  $\eta$ , was varied, and  $h$  was assumed to vary with the strain as described above for the modulus. Strain rates and maximum strain were varied as in the experimental study. Although the strain rate was constant, the variation in  $n$  as the strain changes lead to a varying viscous force in the ligament.

The interaction of the input values and the maximum stress is complex, with nonlinearities with respect to  $\eta$ ,  $\epsilon_0$ , and strain rate. In general, increases in strain rate and damping parameter generate increases in maximum stress, while  $\epsilon_0$  is inversely related to the maximum stress, with the effect being more pronounced in the first cycle. The maximum stress decreased by 19.5% as  $e_0$  varied from 2.5% to 15%. A closer look at the effect of the damping parameter at each strain rate, normalized to the stress for a strain rate of 25%/sec, is presented in Figure 1. The model predictions clearly show a trend similar to the experimental data, with an increase in either strain rate or damping parameter leading to higher stresses. Increasing strain rate from 25 to 100%/sec resulted in the maximum stress increasing by 31%.

The validation and parametric analysis shows that the proposed model is capable of recreating the entire range of stress-strain behavior obtained in previous experimental studies, including the strain rate effects. The maximum stress was calculated for a wide range of strain rate, activation strain, and viscous coefficient. The activation strain was found to have a considerable effect on the overall ligament behavior, and faster rates of load application were associated with the higher stress levels, with the effect being more pronounced in the first loading cycles. Experimental results also indicate increased stiffness and earlier activation with cycling. Energy dissipation exhibited a nonlinear dependence on the viscoelastic parameters and increased as much as five-fold with strain rates varying from 12.5%/sec to 100%/sec. Conversely, larger activation strains (from 5% to 15%) lead to a 60% decrease in the energy dissipation. These effects were present at a smaller scale, but were no less important, at the third and later cycles.

**Intervertebral Discs:** Multiple researchers have performed load tests on single motion segments (vertebrae-disc-vertebrae). The segment level tested, and the reported results, vary from test to test, but the average stiffness over a given load range can be determined from many of the studies. The motion segment stiffness will

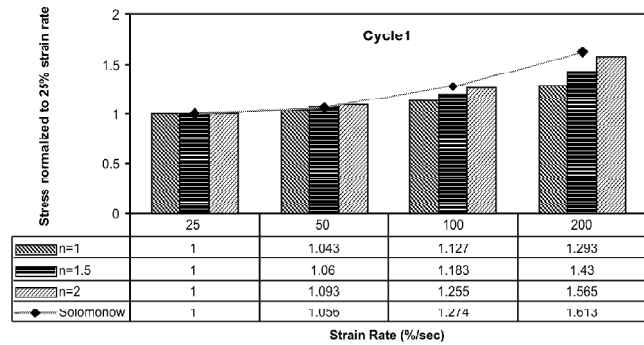


Figure 1: Effect of damping parameter and strain rate on stress predictions using ligament parameters from Cycle 1

therefore be used to compare the developed analytical model to the experimental results. Stiffness values for segments tested in axial compression, shear, and flexion are available and are shown in Table 4. The stiffness reported is the secant stiffness at 1000 N load for compression and shear and 6 N-m for flexion.

Table 4  
Comparison of experimental motion segment stiffness values with model predictions

Study	Axial Compression ( $10^5$ N/m)	Shear ( $10^5$ N/m)	Flexion (N-m/degree)
Schultz (1979)	6.7	1.45	0.9
Markolf (1971)	10.0	-	2.7
Panjabi (1984)	13.0	1.25	1.7
Lavaste (1992)	8.0	-	3.0
Model	11.5	1.44	1.63

The material properties in the model were varied to examine their affect on the response. A set of starting properties were defined based on available data and these were used to establish a baseline value of stiffness for each loading case. The starting material and geometric properties used in the validation study are given in Tables 1 and 5:

Table 5  
Material and geometric properties of structural elements of the lumbar spine used in present FE model

Overall	Vertebral height	30 mm	Disc height	10 mm
Nucleus	$E_{compression}$	10 MPa	$E_{tension}$	1.5 MPa
Annulus	Fiber Content	20%-30%	Fiber $e_0$	2.5%
	Fiber $\psi$	18	Fiber Angle	60 degrees w/Vertical
Facet Joints	Stiffness	200 N/mm		

Axial compression of 1000 N was applied to the model and the resulting stiffness was determined. For the baseline properties, the segment stiffness was  $11.5 \times 10^5$  N/m with the ligaments and  $10.7 \times 10^5$  N/m without the

ligaments. These values were both similar to the experimental data that had a mean of  $9.5 \times 10^5$  N/m and ranged from  $6.7 \times 10^5$  to  $13.0 \times 10^5$  N/m. The relevant material property parameters were varied and the effects on the model results are discussed.

The compression modulus of the nucleus ( $E_n$ ) was ranged from 1.5 MPa to 20 MPa and the stiffness was determined both with and without ligaments as shown in Figure 2. As expected, increasing the nucleus compressive modulus increased the motion segment compression stiffness, and the stiffness with the ligaments present was larger than without the ligaments in all cases.

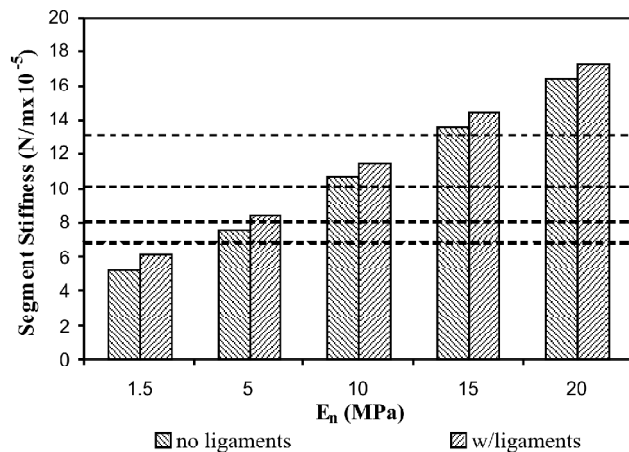


Figure 2: Effect of nucleus modulus variation on the resulting axial stiffness of the motion segment, including experimental results from other studies

In the present model, the nucleus tension modulus was taken as 1.5 MPa while the compression modulus was varied. In a physical disc, the annulus provides confinement to the nucleus, resisting bulging and increasing the axial stiffness. In order to increase the computational efficiency of this model, this stiffening effect is not directly modeled. The lack of direct confinement can be compensated for by increasing the compression modulus of the disc. An approximation of the effect can be determined by assuming (1) the nucleus is incompressible and (2) the annulus is 100% effective at resisting bulging leading to an effective modulus value of about 20 MPa. Since the nucleus is actually somewhat compressible (Iatridis *et al.*, 1996), and the annulus is not completely effective at resisting bulging, a lower value should be expected in practice and is borne out by the results of the validation study.

A parametric analysis of the material properties indicates that the percentage of collagen fiber, transition strain and parameter of the fibers, ground substance modulus, and facet joint stiffness and contact gap had only minor effects on the overall segment stiffness. It was reported in the literature (White and Panjabi, 1990; Bogduk, 1997) that the “normal” fiber orientation is

approximately 60-65 degrees from the disc axis. Smaller values, indicating the fibers are oriented more parallel to the load, lead to increased segment stiffness. The fibers oriented more parallel to the axis are more effective in tension and compression, but also provide less resistance to disc bulging. Since the bulging is not directly modeled the net result in the model is an enhanced resistance to the compressive load. Increasing the percentage of the fibers in the annulus also increased the segment stiffness since the fibers are much stiffer than the ground substance. However, since the fibers are not very active in compression, the effect is fairly small, with an increase from 30% to 50% fiber content only increasing the segment stiffness by 6.8%.

**Shear Behavior:** The model was loaded with an anterior shear of 1000 N resulting in baseline property stiffness of  $1.44 \times 10^5$  N/m and  $0.99 \times 10^5$  N/m with and without ligaments respectively. The experimental data averaged  $1.35 \times 10^5$  N/m with a range of  $1.25 \times 10^5$  to  $1.45 \times 10^5$  N/m. Only changes in the collagen fiber activation strain and stiffness had a significant effect on the shear stiffness (Figure 3). In particular, the activation strain caused a reduction in the stiffness of as much as three times as it varied from 0% to 12%. The collagen modulus had a similar, but somewhat smaller effect, with increasing modulus causing an increase in stiffness. The effect of the modulus change was smaller at higher activation strains. The segment stiffness also increased with the fiber content of the annulus, with the change from 20 to 40% leading to a 27% increase in segment shear stiffness.

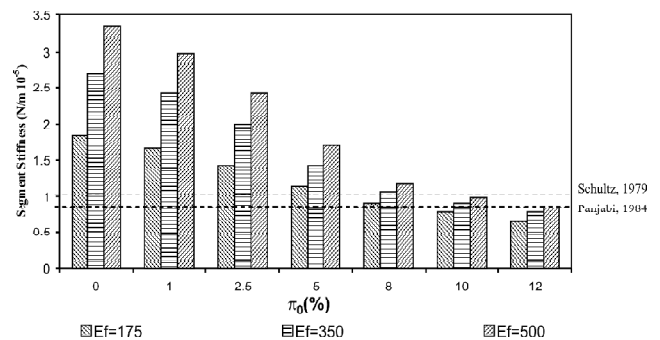


Figure 3: Segment stiffness as a function of initial strain and fiber modulus during shear test, including experimental results from other studies

The ligament contribution to the shear stiffness was about 31% in the baseline case. The contribution of ligamentum flavum had the greatest effect, up to 20%, while the posterior longitudinal ligament increased the segment stiffness by about 12%. Interestingly, for the case of anterior shear, the interspinous ligament did not significantly contribute to the stiffness, even though this ligament is oriented to resist anterior shear. The reason is that the ligament fibers run from near the disc on the

lower vertebrae to near the posterior of the upper ligament (Bogduk, 1997). In this situation, the ligament will act in compression for anterior shear, thus providing little resistance.

**Flexion Behavior:** The model was loaded in flexion with a moment of 6 N-m and the bending stiffness was calculated as 1.63 N-m/deg without ligaments and 2.29 N-m/deg with ligaments for the baseline material properties. The experimental values varied from 0.9 N-m/deg to 3.0 N-m/deg and the baseline results are squarely within the range. The effect of changing the material properties on the segment flexion stiffness is described below.

Variation in the nucleus modulus, both tension ( $E_t$ ) and compression ( $E_c$ ), had little effect on the bending stiffness. In fact, even a 50% change in  $E_c$  led to only a 7.5% change in segment stiffness. This is due to the behavior of both the disc and the model under flexion. Although the location of the center of rotation can vary greatly under combined axial, shear, and flexion loads, under pure flexion loads it tends to be located somewhere near the center of the disc. What this means is that, while the components farthest from the disc center (ligaments, annulus) are highly stressed, the center of the disc has relatively little change in length. Since the model uses a single element located at the disc centroid for the nucleus, that element is only lightly stressed and changing its properties has little effect on the overall results for pure flexion loads.

The variations in annulus properties, however, had a great impact on the overall segment stiffness during the flexion test. The effect of the ground substance modulus shows that larger values lead to stiffer segments. However, the presence of tension in some parts of the annulus, increasing the importance of the fibers, and the large moment arms for the ligaments, decreases the importance of the ground substance. Figure 4 illustrates the influence of both the fiber transition zone center strain and modulus.

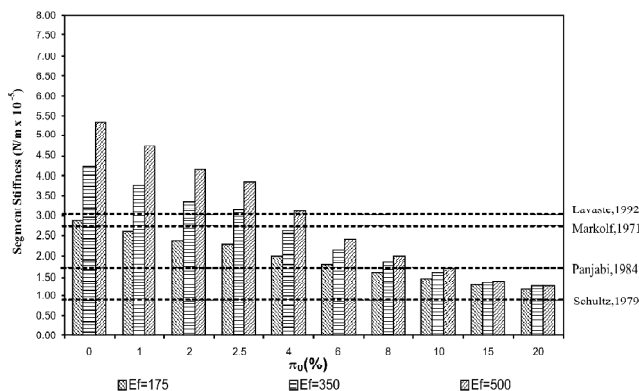


**Figure 4:** Effect of the  $\epsilon_0$  and  $E_f$  on the stiffness of the motion segment with ligaments, including experimental results from other studies

Flexion stiffness decreases as  $\epsilon_0$  grows, and larger fiber moduli lead to stiffer segments in all cases. One interesting observation is that the effect of increasing  $E_f$  diminishes as the activation strain increases. This is because at larger values of  $\epsilon_0$  the fibers essentially never activate, and inactive fibers are not affected by changes in the modulus.

The presence of ligaments contributed about 29% to the segments stiffness for the baseline material properties. All of the ligaments contributed to some degree, with the anterior longitudinal ligament (due to compression) and the interspinous ligament (due to its orientation) having smaller effects. As the significance of the other parameters increased, for example through larger fiber moduli or smaller  $\epsilon_0$ , the stiffness enhancing role of the ligaments diminished. Note that the significance of the ligaments was apparent not only through the stiffness measurements. Instability of the calculation was encountered for some combinations of material properties if the ligaments were absent. This appears to reinforce the notion that a major role of the ligaments is to provide stability to the spine (White and Panjabi, 1990; Gedalia, *et al.*, 1999; Solomonow *et al.*, 1999; Solomonow, 2004).

**Cyclic Loading:** Limited data is available that considers cyclic loading over long periods, as opposed to creep or relaxation loading, and presents sufficient information on the testing methods, specimens, and results as to be useful. The studies by Koeller *et al.* (1984a, 1984b) consisted of axial compression testing of a single motion segment, with ligamentous tissue removed, using a low-rate preload followed by a 1 Hz cyclic load for up to six hours. Force and displacement data were collected and subsequently processed to obtain dynamic stiffness and energy values which will be used for comparison with the current model.

The behavior of the disc changes as the number of cycles increase. The current model uses energy dissipation to vary the material properties, as described in Part I of this paper, to capture these effects. Several input parameters can be varied to change the time-dependent behavior. These include the initial and ultimate modulus for the nucleus, ground substance, and collagen fibers, the reference energy, and the damping coefficients. The initial modulus of the components has been determined in the previously presented validation studies, and based on an examination of the available experimental data, an ultimate modulus twice the initial modulus will be used (Koeller *et al.*, 1984a; 1984b; 1986). However, the reference energy will be varied to determine its effect on the rate of increase in modulus, and the damping parameters will be examined relative to the energy dissipation.

Typical energies for a motion segment tested to failure in a single cycle range from 900 to 6000 mJ

(Adams *et al.*, 1994; Virgin, 1951; Brown *et al.*, 1957; Markolf, 1970). Also, for the loads used in this example, the input energy for a single cycle was approximately 10 mJ. Therefore, a baseline value for the reference energy (30 mJ) was determined by examining the deformation over a six-hour cyclic load and based on the previous energy studies. A baseline damping parameter was also chosen in the same manner. The relative energy in the first cycle was approximately 0.09 in the experiments and similar results (0.091 to 0.123) were obtained by Gardner-Morse and Stokes (2004). A damping coefficient of 0.20 N-s/mm<sup>2</sup> was chosen to approximate this value of relative energy (0.094) in the model.

For the baseline values of reference energy and damping coefficient, the relative deformation and relative energy dissipation are comparable to the experimental values. Creep after six hours was calculated as 1.2 times the initial (preload) deformation. The experimental values of creep varied between 0.75 and 1.6 times the preload deformation. Calculated relative energy was 0.03 per cycle which matched the average experimental value. Parametric analysis of the reference energy indicates that increasing the reference energy has a significant effect on the deformation with a doubling of  $E_{ref}$  leading to an increase in creep of 250%, while have little effect on the dynamic stiffness or relative energy. Increasing  $E_{ref}$  leads to a slower increase in static stiffness and hence larger creeps. Conversely, the damping coefficient had a greater effect on the relative energy (doubling for a 50% increase in damping) while showing only a small effect on the dynamic stiffness and no change in creep.

#### 4. MODEL APPLICATION

**Experimental Design and Data Collection:** As part of the model development and validation, data was collected for a series of sagittal lifts. A 24-year-old male subject was required to repetitively lift a 6.8 kg box while standing on a force plate (Figure 5). The height and weight of the subject were 180 cm and 82 kg respectively. The initial position of the box was at a height of 88 cm above the floor and at a horizontal distance of 74 cm from the center of the force plate. The box, measuring 20 × 20 × 16 cm was lifted from its initial position to approximately waist level at an upright standing posture and then returned to the initial position. Five minutes of motion data was continuously collected for the sagittally symmetric lifting task with a frequency of 6 lifts/min for a total of 60 flexion cycles, with rest between the cycles. The protocol was approved by the Institution Human Subjects Committee and informed consent was obtained from the subject.

**Results:** Validation of the complete model is performed using the experimental setup described above along with other published studies. The results presented



Figure 5: Experimental measurement of lifting motion

in this paper demonstrate the capabilities of the model to predict both overall and detailed behavior.

The variation in centroidal compression force, anterior compressive stress, and posterior tensile stress at the L<sub>4</sub>/L<sub>5</sub> level over the course of a single bending cycle is shown in Figure 6. The peak compressive force of 3636 N, adjusted to account for the active muscle force (Potvin *et al.*, 1991) compares favorably with data presented by Potvin's (1991) model and Wilke's measurements (2001).

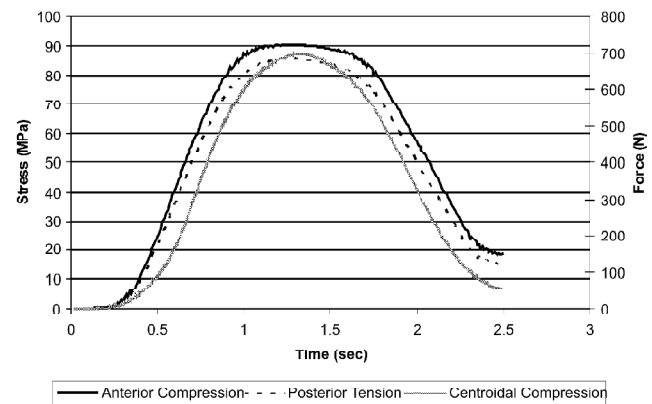


Figure 6: Variation of centroidal compression force, anterior compressive stress, and posterior tensile stress at L<sub>4</sub>/S<sub>1</sub> during a single bending cycle

Peak values of compressive force, posterior tensile stress, and anterior compressive stress, normalized to the values at the L<sub>5</sub>/S<sub>1</sub> level, are shown in Figure 7. The model clearly captures the variation in force by level, including the relative importance of compression and bending. The variation in bending and compression can be seen in Figure 8 which shows the contribution to the total energy dissipation in the discs at two levels, separated by behavior type.

Further evidence of the model's ability to capture detailed results while performing near real-time long term

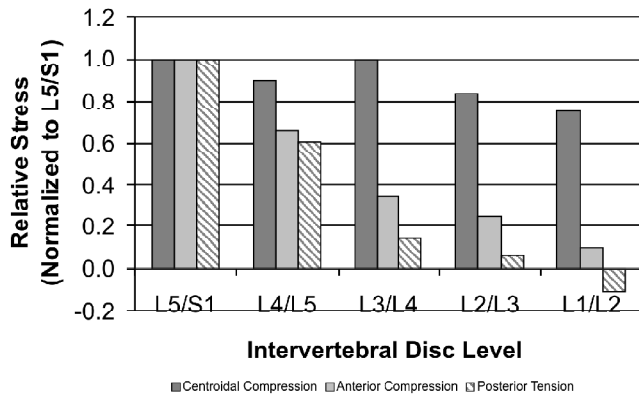


Figure 7: Variation in maximum centroidal compression, anterior stress, and posterior stress by level relative to L5/S1

calculations can be seen in the ligament force predictions. The forces at the  $L_5/S_1$  level for the posterior longitudinal ligament and the ligamentum flavum, and at the  $L_3/L_4$  level for the supraspinous ligament were 5.5 N, 7.3 N, and 190 N respectively. These compare favorably with the values calculated by McGill (1988) for 13 degrees flexion of 6 N, 12 N, and 165 N for the same three ligaments.

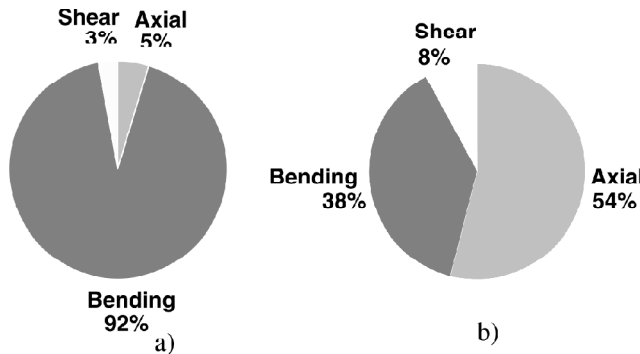


Figure 8: Distribution of energy dissipation source: (a)  $L_5/S_1$  level; (b)  $L_3/L_4$  level

The intervertebral disc forces were significantly different for lifting and lowering tasks. The maximum centroidal compressive force, anterior stress, posterior stress, and anterior/posterior shear for a lowering task, relative to the maximum values for the corresponding lifting task, are shown in Figure 9 for all disc levels. Depending upon spine level, the compressive force, shear, and stresses during lowering ranged from 76 to 107% of the lifting task forces, with smaller decreases seen at the higher disc levels. Note that the posterior stress at  $L_2/L_3$  changes from tension to compression due to smaller rotations during the lowering task.

The energy in the discs is continuously increasing and decreasing as the disc is loaded and unloaded, but over time the energy gradually but steadily increases as seen in Figure 10. This increase is due to the dissipation

of energy that occurs because the energy input into the disc by the loads is not fully recovered. The dissipated energy typically becomes heat generated within the tissue, leads to intercellular matrix reorganization, and drives fluid exchange etc. (Bogduk, 1997; Martin *et al.*, 1998). Examination of the energy dissipation over five minutes of lifting shows that, in comparison to other levels, the  $L_5/S_1$  disc has substantially higher levels of energy dissipation that increase with the modulus. The creep continually increased, but at a decreasing rate, becoming essentially constant near the end of twenty minutes of lifting at a value of 2.3 mm, or approximately 25% of the disc height.

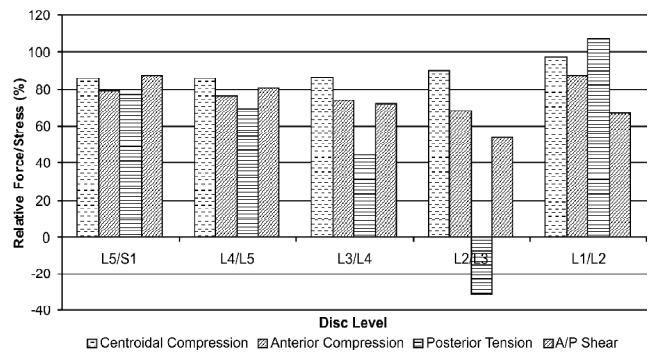


Figure 9: Centroidal compressive force, anterior and posterior stress, and anterior/posterior shear for a lowering task relative to the values for the corresponding lifting task

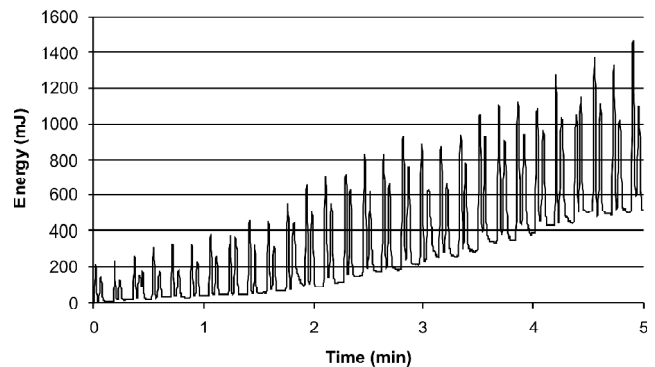


Figure 10: Disc energy variation for  $L_5/S_1$  over five minutes of sagittal lifting and lowering

### 6. DISCUSSION

In general, this model performed well in the validation testing. The component elements were able to accurately predict the desired behavior observed in the experimental results. Using standard material properties and geometry from the literature, the model provided results that were within the scatter of the reported results. In addition, by varying the material properties within their known ranges, the model could reproduce the entire range of observed behaviors. The results obtained for the complete lumbar spine also correlated well with the limited published data.

The model was capable of distinguishing between the behaviors at different levels in the spine. A variation in centroidal compressive force was observed with the compression at L1/L2 at 75% of the value at L5/S1. However, the difference in bending moment was dramatic as seen in the maximum and minimum stress in the discs. The maximum compressive stress at L1/L2 was only 10% of the value at L5/S1, and the posterior region stayed in compression for the entire lift. The difference in behavior was also seen in the energy values with bending dominating the internal energy at L5/S1 (92% of total) and contributing only 38% at L3/L4.

Lifting and lowering tasks are characterized by differing motions of the lumbar spine, even though the starting and ending points are the same. The model was able to predict the difference in forces resulting from the motions. The lowering task generated lower forces in compression and shear, averaging about 20% less than during the lifting task. The ability to distinguish between the behaviors from slightly different motions is crucial to predicting injuries and developing prevention techniques. The results from this study indicate that the model presented is able to accurately capture the forces arising from different, realistic motions.

A limitation of the current model is that the muscle forces are not included in the model and as a result only passive forces are predicted. However, the motion was determined from realistic, subject specific measurements and the passive component of the forces were validated using published results. In addition, the model is two-dimensional and only sagittally symmetric lifts can be analyzed, although the individual component models are easily extended to three dimensions. Finally, further validation of the complete model is required once adequate experimental data becomes available.

## 7. SUMMARY

The model presented in this paper bridges the gap between detailed finite element models and simplified models. The finite element model loading was linked to experimental measurements of the lumbar spine motion during repeated sagittal lifting. Individual component forces and behavior are accurately predicted while maintaining the ability to perform large-displacement nonlinear analyses in near real-time.

The complete model and individual model components have been validated by comparison to experimental results. Individual motion segment response for both static and dynamic loads and ligament behavior were extensively exercised and found to accurately reproduce the experimental data. The model was shown to predict force levels in line with previous studies. In addition, the variation in compression and bending, and their relative importance, between disc levels can be

determined with the model. Detailed results, including the individual ligament forces and anterior/posterior stresses in the disc were obtained, all in near real-time. The ability to rapidly generate and execute models, including linking the model to real-world loading conditions, allows the use of this model in conditions where more traditional analytical models are either too time consuming or of inadequate detail.

## REFERENCES

- [1] Adams, M. A., Green, T. P., Dolan, P., The strength in anterior bending of lumbar intervertebral discs. *Spine* **19**, 2197-2203, 1994.
- [2] Bogduk, N., *Clinical Anatomy of the Lumbar Spine and Sacrum*. Churchill Livingstone, New York, 1997.
- [3] Brown, T., Hanson, R., Yorra, A., Some mechanical tests on the lumbo-sacral spine with particular reference to the intervertebral discs. *J. Bone Joint Surg.* **39A**, 1135, 1957.
- [4] Campbell-Kyureghyan, N., *Computational analysis of the time-dependent biomechanical behavior of the human lumbar spine*. PhD thesis, Ohio State University Press, Columbus, 2004.
- [5] Campbell-Kyureghyan, N., Jorgensen, M., Burr, D., Marras, W., The prediction of lumbar spine geometry: method development and validation. *Clinical Biomechanics*, **20**(5), 455-464, 2005.
- [6] Chazal, J., Tanguy, A., Bourges, M., Gaurel, G., Escande, G, Guillot, M., Vanneuville, G., Biomechanical properties of spinal ligaments and a histological study of the supraspinal ligament in traction. *Journal of Biomechanics*, **18**(3), 167-176, 1985.
- [7] Ezquerro, F., Simon, A., Prado, M., Perez, A., Combination of finite element modeling and optimization for the study of lumbar spine biomechanics considering the 3D thorax-pelvis orientation. *Medical Engineering and Physics*, **26**, 11-22, 2004.
- [8] Fagan, M. J., Julian, S., Siddall, D. J., Mohsen, A. M., Patient-specific spine models. Part 1: finite element analysis of the lumbar intervertebral disc-a material sensitivity study. Proceedings of the Institution of Mechanical Engineers Part H: *Journal of Engineering in Medicine*, **216**, 299-314, 2002.
- [9] Gardner-Morse, M. G., Stokes, I. A. F., Structural behavior of human lumbar spinal motion segments. *J Biomechanics*, **37**, 205-212, 2004.
- [10] Gedalia, U., Solomonow, M., Zhou, B. H., Baratta, R. V., Lu, Y., Harris, M., Biomechanics of increased exposure to lumbar injury caused by cyclic loading. Part 2. Recovery of reflexive stability with rest. *Spine*, **24**, 2461-2467, 1999.
- [11] Goel, V. K., Park, H., Kong, W., Investigation of vibration characteristics of ligamentous lumbar spine using the finite element approach. *Journal of Biomechanical Engineering*, **116**, 377-383, 1994.
- [12] Iatridis, J. C., Weidenbaum, M., Setton, L. A., Mow, V. C., Is the nucleus pulposus a solid or a fluid? Mechanical behaviors of the nucleus pulposus of the human intervertebral disc. *Spine* **21**(10), 1174-1184, 1996.
- [13] Koeller, W., Meier, W., Hartmann, F., Biomechanical properties of human intervertebral discs subjected to axial dynamic compression. A comparison of lumbar and thoracic discs. *Spine* **9**, 725-733, 1984a.
- [14] Koeller, W., Funke, F., Hartmann, F., Biomechanical behavior of human intervertebral discs subjected to long lasting axial loading. *Biorheology*, **21**, 675-686, 1984b.

- [15] Koeller, W., Meier, W., Hartmann, F., Biomechanical properties of human intervertebral discs subjected to axial dynamic compression – influence of age and degeneration. *Journal of Biomechanics*, **19**, 807-16, 1986.
- [16] Kong, W. Z., Goel, V. K., Gilbertson, L. G., Prediction of Biomechanical parameters in the lumbar spine during static sagittal plane lifting. *Journal of Biomechanical Engineering* **120**, 273-280, 1998.
- [17] Kunnath, S. K., Chai, Y. H., Cumulative damage-based inelastic cyclic demand spectrum. *Earthquake Engineering and Structural Dynamics*, **33**, 499-520, 2004.
- [18] Lavaste, F., Skalli, W., Robin, S., Camille, R., Mazel, C., 3D geometrical and mechanical modeling of the lumbar spine. *Journal of Biomechanics*, **25**, 1153-1166, 1992.
- [19] Lee, U., A theory of continuum damage mechanics for anisotropic solids. *Journal of Applied Mechanics*, **66**, 264-8, 1999.
- [20] Lee, C., Kim, Y. E., Lee, C. S., Hong, Y. M., Jung, J., Goel, V. K., Impact response of the intervertebral disc in a finite element model. *Spine*, **25**, 2431-2439, 2000.
- [21] Lu, Y. M., Hutton, W. C., Gharpuray, V. M., Do bending, twisting, and diurnal fluid changes in the disc affect the propensity to prolapse? A viscoelastic finite element model. *Spine*, **21**, 2570-2579, 1996.
- [22] Markolf, K. L., Deformation of the thoracolumbar intervertebral joints in response to external loads. *Journal of Bone and Joint Surgery*, **54**, 511-533, 1971.
- [23] Martin, R. B., Burr, D. B., Sharkey, N. A., *Skeletal Tissue Mechanics*. Springer, New York, 1998.
- [24] McGill, S. M., Estimation of force and extensor moment contributions of the disc and ligaments at L4-L5. *Spine* **13**, 1395-1402, 1988.
- [25] Nordin, M., Frankel, V. H., *Basic Biomechanics of the Musculoskeletal System*. Lippincott Williams and Wilkins, Baltimore, 2001.
- [26] Panjabi, M. M., Krag, M. H., Chung, T. Q., Effects of disk injury on mechanical behavior of the human spine. *Spine*, **9**, 707-713, 1984.
- [27] Pankoke, S., Buck, B., Woelfel, H. P., Dynamic FE model of sitting man adjustable to body height, body mass and posture used for calculating internal forces in the lumbar vertebral disc. *Journal of Sound and Vibration*, **215**, 827-839, 1998.
- [28] Potvin, J. R., McGill, S. M., Norman, R. W., Trunk muscle and lumbar ligament contributions to dynamic lifts with varying degrees of trunk flexion. *Spine*, **16**, 1099-1107, 1991.
- [29] Schultz, A. B., Warwick, D. N., Berkson, M. H., Nachemson, A., Mechanical properties of human lumbar spine motion segment – Part I: Responses in flexion, extension, lateral bending and torsion. *Journal of Biomechanical Engineering*, **101**, 46-52, 1979.
- [30] Shah, J. S., Jayson, M. I. V., Hampson, W. G. J., Low tension studies of collagen fibers from ligaments of the human spine. *Ann Rheum Dis*, **36**, 139-148, 1977.
- [31] Shah, J. S., Structure, morphology and the mechanics of the lumbar spine. In Jayson, M. (ed). *The Lumbar Spine and Backache*, 2<sup>nd</sup>. ed. Pitman, London., Ch. 13, 1980.
- [32] Shirazi-Adl, A., Ahmed, A. M., Shrivasta, S.C., Mechanical response of a lumbar motion segment in axial torque alone and combined with compression. *Spine*, **11**, 914-927, 1986.
- [33] Solomonow, M., Zhou, B., Baratta, R. V., Lu, Y., Harris, M., Biomechanics of increased exposure to lumbar injury caused by cyclic loading: Part 1. Loss of reflexive muscular stabilization. *Spine*, **24**, 2426-2434, 1999.
- [34] Solomonow, M., Ligaments: a source of work-related musculoskeletal disorders. *Journal of Electromyography & Kinesiology* **14**, 49-60, 2004.
- [35] Tkaczuk, H., Tensile properties of human lumbar longitudinal ligaments. *Acta Orthopaedica Scandinavica Supplement* **115**, 1-69, 1968.
- [36] Virgin, W., Experimental investigations into physical properties of intervertebral disc. *J. Bone Joint Surg.* 33B, 607, 1951.
- [37] White, A. A., Panjabi, M. M., *Clinical Biomechanics of the Spine*, 2<sup>nd</sup> edition, Lippincott Company, Philadelphia, 1990.
- [38] Wilke, H., Neef, P., Hinz, B., Seidel, H., Claes, L., Intradiscal pressure together with anthropometric data—a data set for the validation of models. *Clinical Biomechanics* 16 Supplement 1, S111-S126, 2001.
- [39] Yoshida, J., Abe, M., Fujino, Y., Constitutive Model of High-Damping Rubber Materials. *Journal of Engineering Mechanics* **130**, 129-41, 2004.